Comparison between Frequency Selective Surfaces with Rectangular and Hexagonal Periodicity Operating as Absorbers

Aldo De Sabata
Dept. of Measurements and Optical Electronics
Politehnica University Timisoara
Timisoara, Romania
aldo.de-sabata@upt.ro

Ovidiu Zeno-Lipan
Dept. of Physics
Uniersity of Richmond
Richmond, USA
olipan@richmond.edu

Ladislau Matekovits
Dept. of Electronics and Telecommunications
Politecnico di Torino
Torino, Italy
ladislau.matekovits@polito.it

Andrei-Marius Silaghi
Dept. of Measurements and Optical Electronics
Politehnica University Timisoara
Timisoara, Romania
andrei.silaghi@upt.ro

***Abstract*—Two frequency selective surfaces operating as absorbers, with rectangular and hexagonal periodicity respectively, and relying on the same metal pattern in the unit cell are compared. The structures are implemented on an FR4 substrate, covered with copper metallization. The frequency responses (reflection coefficient) in normal incidence of electromagnetic waves and contents of higher order modes in the two cases are compared. Finally, the frequency response in oblique incidence of the hexagonal array is reported.**

Keywords—FSS, absorber, reflection coefficient

I. Introduction

Absorbers are thin layers of (meta)materials devised for preventing reflection of electromagnetic waves in view of applications to stealth technology and to protecting enclosures from radiation of or exposure to electromagnetic waves in certain frequency bands.

Frequency selective surfaces (FSSs) have been considered as an appropriate solution for designing absorbers for a long time now [1], and are still considered of interest, as demonstrated by the large number of research teams involved in this topic (see [2-6] to quote just a few of the most recent). A convenient design for FSS absorbers relies on impressing a periodic metallic pattern on one side of a printed circuit board and applying a continuous metallization on the other side.

FSSs result by periodic repetition of a unit cell along different lattice axes. Most commonly, the resulting array have rectangular or hexagonal periodicity. The latter case raised attention to researchers due to the possibility of a more compact packing of the unit cell pattern repetition [7-11]. Sub-wavelength dimensions of the unit cell allow for increased insensitivity to incidence angle, while symmetry favors a polarization-independent response of the FSS.

The intrinsically lossy nature in the materials involved in the construction of the FSS contributes to dissipation of the absorbed electromagnetic energy. Nevertheless, higher order modes may be launched on the FSS which may re-radiate energy when encountering discontinuities such as the edges of the finite experimental implementation of the FSS.

In this paper, a comparison between two FSSs that are obtained from the same metallization of the unit cell is presented. One solution involves rectangular (square) periodicity, while the other one relies on hexagonal grid. Both FSSs are implemented on an FR4 substrate. The face opposed to the periodic pattern is covered with metal to prevent transmission of electromagnetic waves. The comparison is made in terms of reflection coefficient and contents of higher order modes. An assessment of the response of the FSS with hexagonal periodicity for oblique incidence is also considered.

This paper is organized as follows. In Sec. II, the designs of the FSSs are described. In Sect. III, the responses of the two structures to electromagnetic waves in normal incidence operation are compared and discussed. The response of the FSS with hexagonal periodicity for oblique incidence of electromagnetic waves is reported and commented in Sec. IV. Conclusions are drawn in the last Section.

II. Presentation of Structures

The structures are based on the unit cell presented in Fig. 1.

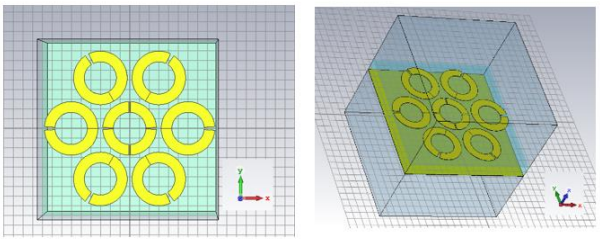

(a) (b)

Fig. 1. CAD model of the unit cell. Metal pattern (yellow) on the upper part: (a) Front view, and (b) 3D perspective view.

The metal pattern (within the single unit cell) impressed of the FR4 substrate (ε_r=4.3, tanδ=0.025), of 1.8 mm thickness, consists of 7 split ring resonators made of annealed copper, having a thickness of 0.035 mm. The external radius of the

resonators is 2.76 mm, the split angle is 8°, and the width of the trace is *w*, to be reported below.

The resonators are arranged in a hexagonal pattern in the unit cell, with the edge of the hexagon measured between the centers of the resonators being equal to 6 mm. An additional resonator is placed at the center of the hexagon, having the same radius and trace width as the resonators arranged in the hexagonal pattern. However, four splits have been cut still preserving the symmetry of the structure.

The other side of the substrate is completely covered with copper to prevent penetration of electromagnetic waves incident from the positive *z* axis (with respect to the reference frame in Fig. 1) into the space below.

FSSs are obtained from the considered unit cell by hexagonal (Fig. 2 (a)) or rectangular (square, Fig. 2 (b)) periodic repetition in the *x*O*y* plane. Each single edge of the hexagon that covers a period of the structure from Fig. 2 (a) is 10 mm, so that the area of the period is 259.8 mm^2. The edge of the square-shaped spatial period of the structure in Fig. 2(b) is 18 mm, resulting in an area of the unit cell of 324 mm^2. The hexagonal pattern versus the square pattern allows for a denser packing of the basic pattern from Fig. 1 (a).

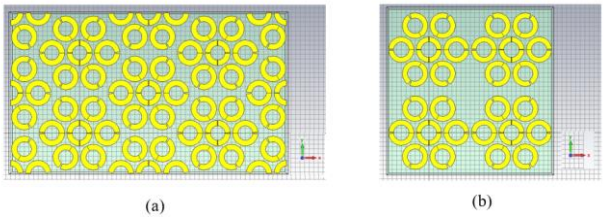

Fig. 2. Array having (a) hexagonal and (b) rectangular periodicity obtained by repetition of the unit cell pattern from Fig. 1 in the xOy plane. Four-unit cells are represented in each panel.

III. Normal Incidence of Electromagnetic Waves

A simulation of plane wave incidence on the hexagonal structure has been performed using an electromagnetic CAD software [12], having the copper trace width *w* as a parameter. Plane wave ports and periodic boundary conditions have been imposed in simulations. The results are reported in Fig. 3.

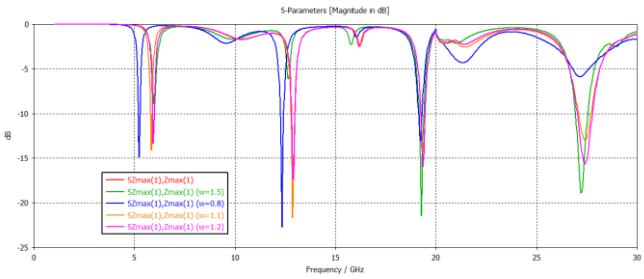

Fig. 3. Reflection coefficient in normal incidence for the hexagonally patterned surface.

Figure 3 reveals that four absorption frequencies are present. To keep a balance between the amplitudes of the notches, a value of the trace width *w*=0.2 mm has been selected, which will be kept constant from now on (only notches lower than -10 dB are considered).

The response in normal incidence of the rectangular array is represented in Fig. 4. This time five notches and a wide stopband are present, apparently providing more design opportunities than the hexagonal counterpart. However, since the dimensions of the structures are not small as compared to the wavelengths involved, an analysis concerning higher order modes is necessary.

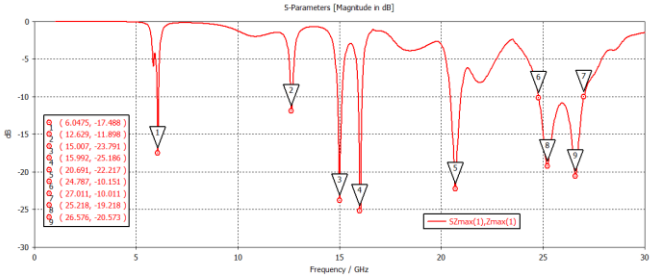

Fig. 4. Reflection coefficient in normal incidence for the square patterned array.

In Fig. 5, the relevant modes associated with the hexagonal structure are reported, and in Fig. 6 the relevant modes for the square array are represented. A number of 60 modes have been considered in the simulations. The *S* parameters for the evanescent modes have been calculated at a distance of 1.8 mm above the structure in order to assess the contribution of the surface waves to the scattered field.

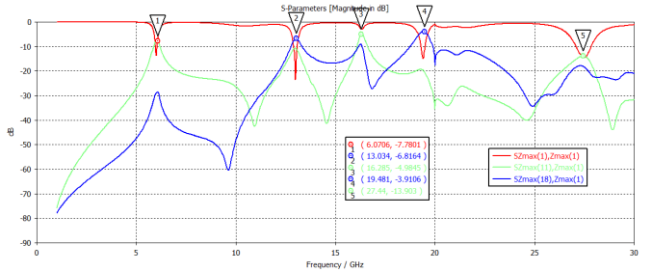

Fig. 5. Reflection coefficient in normal incidence for the hexagonal patterned array with higher order modes included.

Mode 11 (TE 2,0) is evanescent at the frequencies denoted by 1 and 3 in Fig. 5, with attenuation constants of 399.072 and 240.22 m^{-1} respectively and propagative at point 5, with a propagation constant of 394.668 m^{-1}. The mode TE -2,0 has the same parameters due to the normal incidence, a fact that also holds for the modes considered in the rest of this section.

Mode 18 (TM 1,-1) is evanescent at point 2, with an attenuation constant of 317.552 m^{-1}, and mode 20 (TM -1,1) is evanescent at point 4, where the attenuation constant is 99.878 m^{-1}. To conclude, a propagating mode is present only at point 5 (27.44 GHz). However, the transmission coefficient is below -10 dB.

A similar calculation for the square patterned structure yields the results reported in Fig. 6. Mode 4 (TM 0,-1) is evanescent at points 2 and 3 in Fig. 5, with attenuation constants of 227.328 and 153.9 m^{-1} respectively. Mode 9 (TE -1,0) is evanescent at points 1 and 2, with attenuation constants of 327.228 and 93.5401 respectively, and it is propagative at point 5, having a propagation constant of 408.977 m^{-1}. Note that the reflection coefficient of the propagative mode is above -10 dB in this case.

In conclusion, in both cases, special measures have to be taken to prevent radiation of surfaces waves from discontinuities, such as the edges of the finite-dimension structure used in practical applications. The amplitudes of the evanescent waves are in general smaller in the case of the hexagonal pattern as compared to the square one. Both structures reflect some propagating higher order modes when

exposed to similar incident conditions. The reflectance is below -10 dB in the case of the hexagonal pattern, but exceeds -10 dB when the square pattern is used.

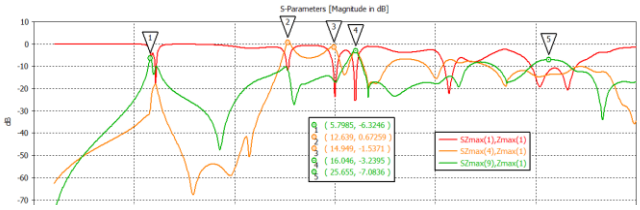

Fig. 6. Reflection coefficient in normal incidence for the square patterned array with higher order modes included.

IV. Oblique Incidence

The hexagonal array has also been tested for reflectance in oblique incidence. The results are reported in Fig. 7.

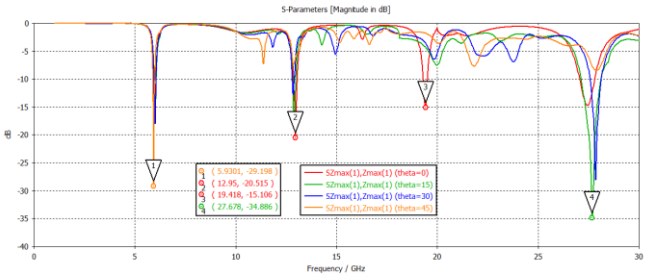

Fig. 7. Reflection coefficient of the hexagonal array for several values of the colatitude angle theta.

As revealed by the graphs in Fig. 7, out of the four stopbands, the first two, situated at lower frequencies, are stable up to an incidence angle of 45º, while the larger stopband situated at the highest frequency can be relied upon up to an incidence angle of 30º, and the band limits slightly change with the incidence angle. Note that the notches become deeper at oblique incidence than at normal incidence for points 1 and 4 in Fig. 7. The notch at point 3 vanishes at oblique incidence.

V. Conclusions

Two FSSs operating as absorbers have been proposed in this paper. Although these FSSs share the same unit cell pattern, they show different scattering behaviors given that the unit cell was hexagonally extended in one case whereas a square extension was used for other one. Both structures have been assessed and compared by full-wave simulation. An analysis of the relevant propagating and evanescent modes has been proposed.

The array with hexagonal periodicity proved to have better applicability as an absorbing structure. The hexagonal structure has been tested in oblique incidence of electromagnetic plane waves. It has been shown that some of the resonant frequencies are stable when the angle of incidence is varied between 0 and 45º. At high frequency, the stability of the notch frequencies has been limited to 30º.

Acknowledgment

This work was supported by a grant of the Ministry of Research, Innovation and Digitization, CNCS - UEFISCDI, project number PN-III-P1-1.1-PD-2021-0010, within PNCDI III.

References

[1] B.A. Munk, Frequency Selective Surfaces - Theory and Design, New York: Wiley, 2000

[2] J. Xing, D. Li, G. Liu, X. Lin, R. Li, R. Zhang, H. Chen, and E.-P. Li, “Ultra-Thin SSPP-Based Sheet for Suppressing Microwave Radiated Emission in SiP Modules”, IEEE Trans. Electromag. Compat., vol. 65, no. 2, pp. 376-385, Apr. 2023.

[3] C. Zhang, S. Xiao, Z. Yao, Z. Jiang, and Y. Li, “On the Design of Ultralow-Profile Broadband Absorber Based on Non-Foster Circuit”, IEEE Antennas Wireless Propag. Lett., vol. 21, no. 3, pp. 600–604, Mar. 2022.

[4] M.A. Shukoor, S. Dey, and S.K. Koul, “A Simple Polarization-Insensitive and Wide Angular Stable Circular Ring Based Undeca-Band Absorber for EMI/EMC Applications”, ”, IEEE Trans. Electromag. Compat., vol. 63, no. 4, pp. 1025-1034, Aug. 2021.

[5] S. Hannan, M.T. Islam, N.M. Sahar, K. Mat, M.E.H. Chowdhury, and H. Rmili, “Modified-Segmented Split-Ring Based Polarization and Angle-Insensitive Multi-Band Metamaterial Absorber for X, Ku and K Band Applications”, IEEE Access, vol. 8, pp. 144051-144063, 2020.

[6] P. Garg, and P. Jain, “Novel Ultrathin Penta-Band Metamaterial Absorber”, AEÜ – Int. J. Electron. Commun., vol. 116, 153063, pp. 1-8, 2020.

[7] Q. Guo, Z. Li, J. Su, L.Y. Yang, and J. Song, “Dual-Polarization Absorptive/Transmissive Frequency Selective Surface Based on Tripole Elements”, IEEE Antennas Wireless Propag. Lett., vol. 18, no. 5, pp. 961–965, May 2019.

[8] X. Zhang, W. Wu, J. Huang, W. Zhang, Y. Te, and N. Yuan, “Dual-Polarized Frequency Selective Rasorber With Two Transmission Bands”, IEEE Access, vol. 7, pp. 139795-139801, 2019.

[9] J.A, Vasquez-Peralvo, J.M. Fernandez-Gonzales, J.M. Rigelsford, and P. Valtr, “Interwoven Hexagonal Frequency Selective Surface: An Application for WiFi Propagation Control”, IEEE Access, vol. 9, pp. 111552-111566, 2021.

[10] Q. Chen, D. Sang, M. Guo, and Y. Fu, “Miniaturized Frequency-Selective Rasorber With a Wide Transmission Band Using Circular Spiral Resonator”, IEEE Trans. Antennas Propag., vol. 67, no. 2, pp. 1045-1052, Feb. 2019.

[11] X. Sheng, J. Ge, K. Han, and X.-C. Zhu, “Transmissive/Reflective Frequency Selective Surface for Satellite Applications”, IEEE Antennas Wireless Propag. Lett., vol. 17, no. 7, pp. 1136–1140, July 2018.

[12] CST, Computer Simulation Technology (v2023).